International Journal of Nanoelectronics and Materials

In Press, Accepted Manuscript – Note to user

Optical Investigations of GaN Nano Films Deposited Using Pulsed Laser Ablation in Ethanol

Husam Aldin A. Abdul Amir[1], Makram A. Fakhri[1,*], Ali. A.Alwahib[1], Evan T. Salim[2,*]

[1]Laser and Optoelectronic department, University of Technology-Iraq
[2]Applied science department, University of Technology-Iraq

Received 29 September 2021, Revised 27 Dec 2021, Accepted 4 January 2022

ABSTRACT

We provide an optical study on GaN thin film testing created by pulsed laser (ablation) in liquid. This study applied six different energies for ablated GaN Nanoparticles in the liquid. According to the XRD test, the diffraction peak (0002) has a narrow FWHM magnitude of 0.12, and the high order GaN diffraction peak has a low FWHM magnitude of 0.12. (0004). The optical range information was used to determine the band gap of samples with discernible crystallinity. Longtails were watched underneath the optical band gaps. Samples are entirely dependent on the laser ablation preparation's energies. The samples with the greatest laser power, 2000 mJ, decreased near band edge emission, peaking at 3.32 eV at room temperature. The largest energy band gap of 3.62 eV was reported at 1400 mJ. As is clear from the results *we obtained, the possibility of using the prepared thin Nano-films in optoelectronics applications such as optical detectors, solar cells, and optical sensors.*

Keywords: Gallium nitride; Pulsed Laser Ablation; energy bandgap; X-Ray Diffraction (XRD); Optical properties; Structural properties.

1- INTRODUCTION

Due to their exceptional physical and optical properties, nanostructured Gallium nitride (GaN) materials have lately received much attention. GaN is a semiconductor with a direct broad bandgap of (3.4 eV) and an excitation binding energy of 26 meV.

GaN has been extensively researched because of its potential application in sensing devices [5, 6]. In addition to short-wavelength electroluminescence applications, GaN-based heterostructure field-effect transistors (HFET) and high electron mobility transistors (HEMT) are constantly popular [7, 8]. GaN may be employed for detectors, short-wavelength optoelectronic devices, and UV or blue region emitters because of its distinct luminosity and longevity compared to light-emitting diodes [9, 10]

The purity of GaN nanoparticles is critical for optoelectronic devices, as it determines their suitability as dynamic regions inside color-tunable light-emitting diodes and their direct broad bandgaps for laser diodes. Multiple techniques have been used to make GaN-based nanoparticles,

*For correspondence; Tel. + (964) 7702793869, E-mail: mokar@yam_76hoo.com, & makram.a.fakhri@uotechnology.edu.iq.
*For correspondence; Tel. + (964) 7715752087, E-mail: evan_tarq@yahoo.com, & evan.t.salim@uotechnology.edu.iq.

Note: Accepted manuscripts are articles that have been peer-reviewed and accepted for publication by the Editorial Board. These articles have not yet been copyedited and/or formatted in the journal house style.

including molecular beam epitaxy (MBE), electrochemical, pulsed laser deposition, chemical vapor deposition (CVD), RF sputtering, spin coating, and other approaches. [11-22]. In any event, most of these plans rely on temperature forms and expensive chemicals. The ability to build high vacuum thin films at low substrate temperatures and a fast growth rate of the pattern of /pulse is reasonably straightforward in pulsed laser technology [23-26].

Almost all commercially available semiconductor III-nitrides are made via heteroepitaxial growth employing molecular beam epitaxy, Pulsed Laser Deposition, MOCVD, and HVPE [27-34]. Although the previously described procedures may be used to prepare, develop, and deposit high-quality Gallium nitride semiconductor layers, these ways of growing to entail complex and sophisticated technologies that are somewhat expensive and difficult to set up [35-38].
Furthermore, several reported procedures for deposition semiconductor III-nitrides nanostructures. The hydride vapor phase epitaxy technique and metal-organic chemical vapor deposition contain hazardous and combustible precursors [39-42]. Following that, scientific researchers must pay close attention to equipment and maintenance costs, chemical waste management, and chemical safety, among other things [43-46].

GaN thin film growth findings were reported by Vinegoni et al. [47] using pulsed laser deposition. Over the whole tested area, this study group developed thin coatings with moderate homogenous dispersed granular formations. Vispute et al. [48] have demonstrated high-level crystallinity on the Al2O3 [0001] substrate surface. L. Goswami et al. Using Au-GaN-NS, a UV Photodetector was created. GaN-NSs were produced on a Si (111) substrate utilizing a PAMBE setup that included an RF plasma source and a Knudsen cell that provided active nitrogen species and gallium metal. The research shows that NS with lower stress-strain, no buffer layer, low aspect ratio, and compatibility with Si-technology can usher in a new age of more cost-effective future nanosensors [49]. Y. Pal et al. Manufacture and description of a thin film of gallium nitride deposited on a sapphire substrate for electrochemical water splitting applications. A chemical vapor deposition (CVD) approach was used to create GaN thin films on a sapphire (Al_2O_3) substrate. In comparison to RHE, the greatest photoconversion efficiency and photocurrent density were 0.73 percent and 0.099mA/cm^2, respectively, at 0.59V [50].

Due to the importance of the GaN in most electronics applications, it is necessary to find safe, simple, and inexpensive methods for growing thin film. Pulsed laser deposition and pulsed laser ablation in the liquid technology have high efficiency, a successful alternative way. This research paper will present a new and safe technology using a standard GaN wafer.

2- EXPERIMENTAL DETAILS

The GaN target was submerged in a 5ml ethanol solution in this experiment. [(Figure 1(a))] A GaN target was fired using a Nd:YAG pulsed laser. A single wavelength (532 nm) and frequency were used to precisely display laser properties (4 Hz). Six samples were produced for each flowing energy of 2000 mJ, 1800 mJ, 1600 mJ, 1400 mJ, 1200 mJ, and 1000 mJ. Each sample was bombarded with 500 pulses to ensure that the fluid was wholly saturated with nanomaterials. The focal length was 12 cm, which changed every 100 pulses to maintain the same GaN and laser surface contact. The ablation approach using a Nd:YAG pulsed laser in a liquid environment is shown in Figure 1(b).

Note: Accepted manuscripts are articles that have been peer-reviewed and accepted for publication by the Editorial Board. These articles have not yet been copyedited and/or formatted in the journal house style.

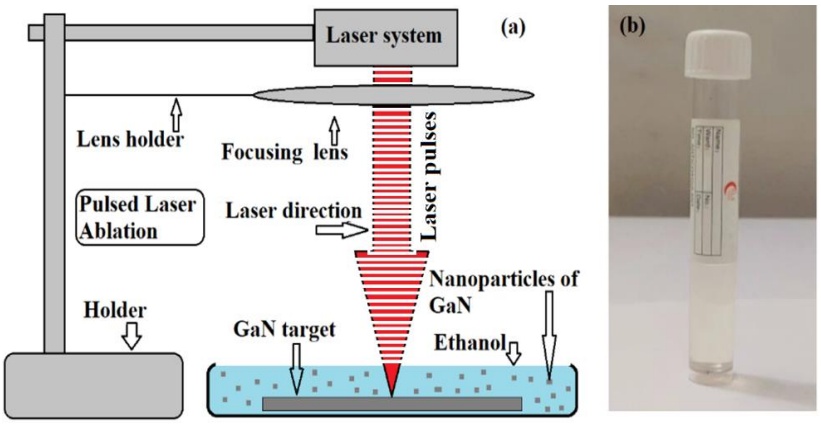

FIGURE 1. a) pulsed laser interaction method b) liquid sample generated from ablation method

The GaN liquid was deposited on the quartz substrate samples using a drop-casting process. A hotplate was used to heat the quartz substrate to a temperature of between (70 °C -90°C). One hundred drops of GaN were deposited to build a thin layer of GaN on the quartz substrate. The water pool is the most considerable side effect of this type of deposition and can be reduced or eliminated by controlling the time interval between each drop. The quartz substrate was used as a basis for Nano-liquid that fell gently and when it reached the required temperature. Before beginning the Alcohol dropping procedure, the quartz substrate was carefully cleaned. The GaN particles in the liquid should not collect at the bottom; the liquid should be agitated before each drop to ensure that the GaN nanostructures are distributed evenly across all samples. The X-Ray Diffraction test was used to evaluate quartz/nanoparticles (GaN) samples for absorption, transmission, and analysis to determine the GaN energy gap.

3- RESULTS AND DISCUSSIONS

3.1 XRD results

Figure 2 shows the XRD patterns of GaN nanoparticles. GaN is used to split the distinctive peaks. Using a Philips X-ray diffraction meter, the XRD pattern of GAN thin films was computed in the 2=20-80 degree range. The film contains firm GaN 32.11, 34.04, 36.82, 48.24, 58.33, 68.86, and 72.85 peaks, which correspond to about the hexagonal plane of GaN of (100) (002) (101) (102) (110) (112) (004) respectively (PDF code: 01-076-0703 [51, 52]), (PDF code: 01-079-2499 [53, 54]), all of the Nano GaN peaks that were evaluated and reported were consistent with prior findings [55, 56]. On the other hand, X-ray diffraction studies revealed that the GaN nano-colloidal had a mono-crystalline structure at various levels. It should be noticed that the majority of the peaks on the show have changed somewhat.
On the other hand, these shifts and transformations occur as a result of flaws or impurities in GaN thin films during the growing process. D = 0.9/ (cos), where d is the diameter of the crystallite grain, is full width at half maximum (FWHM), incident wavelength (0.154 nm), and is the reflection angle, according to Scherrer's Formula. The diffraction peaks have a small FWHM magnitude of 0.12, and the high order GaN diffraction peak shows that the GaN nano-thin films formed on the quartz substrate are of exceptional quality [57-59]. The crystal size values (D) for the nano-film, on the other hand, were computed. The FWHM values dropped with an increase in the crystal size of the thin film nanofibers and an improvement in the quality of the GaN thin film nanoparticle crystals. They varied between 7 and 20 nm from the maximum intensity to the peak.

Note: Accepted manuscripts are articles that have been peer-reviewed and accepted for publication by the Editorial Board. These articles have not yet been copyedited and/or formatted in the journal house style.

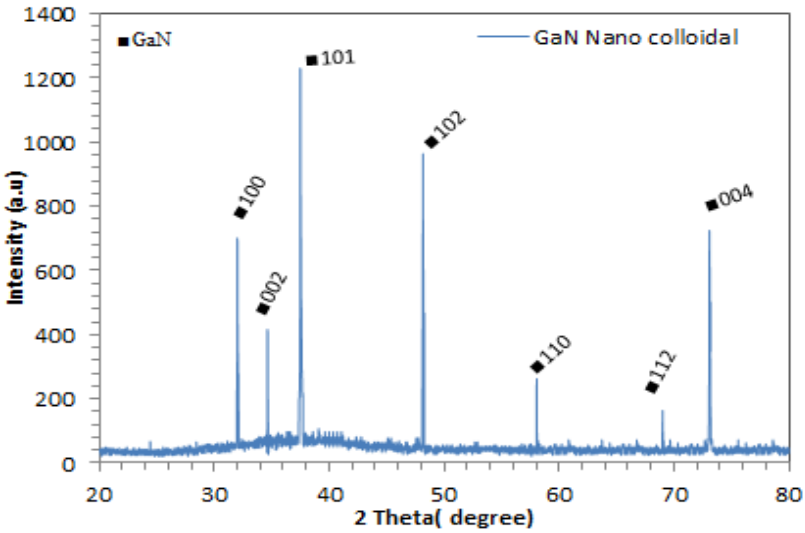

Figure 2. XRD pattern of GaN nanoparticles

3.2 TEM results

Figure 3 displays a TEM picture with a magnification of 100 nm. It is evident from the image of Figure 3 that the particles form are primarily spherical and have an average diameter is between 5 and 70 nm. These findings suggest that the nanoparticles' surface consists of relatively big particles (50-70 nm in diameter) combined with smaller particles (5-10 nm in diameter). Even though few Nanocluster formations emerged in the picture and were connected with the XRD spectrum, the nanoparticles seemed distributed at the matrix.

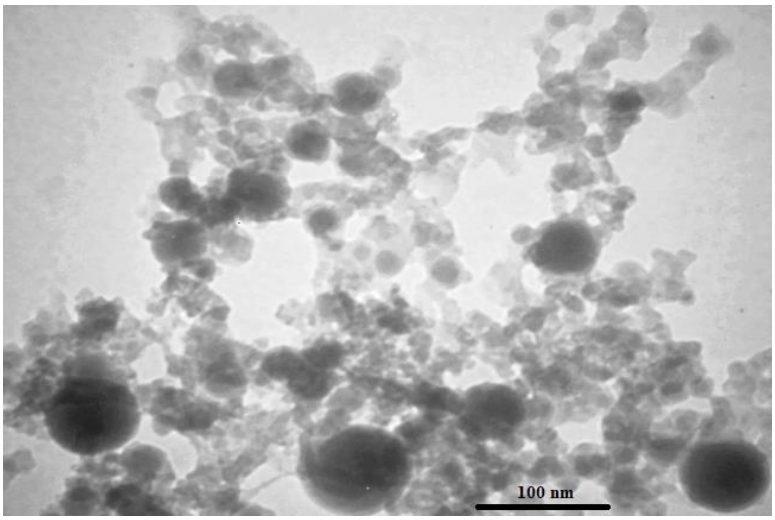

FIGURE 3. TEM image of GaN nanoparticles

3.3 Optical results

Optical properties such as absorptions, absorption coefficients, and transmission as a function of wavelengths in nanometer were tested and calculated using a double beam UV-VIS spectrophotometer over the wavelength range of 300-1100 nm well as the value of the energy bandgap as a function of optical energy.

Note: Accepted manuscripts are articles that have been peer-reviewed and accepted for publication by the Editorial Board. These articles have not yet been copyedited and/or formatted in the journal house style.

The incident photon energy was calculated using the formula (1) [60-64]:

$$E_g\ (eV) = 1.24 / \lambda\ (\mu m) \quad (1)$$

Where Eg is the optical energy gap, and λ is the wavelength of the incident photon. The absorption coefficient was drawn as a function of wavelengths, and the following formula was used to estimate (2) [65-68]:

$$(\alpha h\nu) = B\ (h\nu - Eg)^{r} \quad (2)$$

Where (α) is the calculated absorption coefficient value, hν the energy of the photon, (B) is constant, and (r) is a constant, its values depend on the type of material.

The optical band gap was deduced from the linear relation (extrapolation of the straight line) of the curve between (α hν)1/r and (hν). Following eq. (3) was used to estimate the absorption coefficient at a specific wavelength [69-72]:

$$\alpha = 2.303\ (A / t) \quad (3)$$

A = absorptance and, t = thickness.

The sharp edge at the UV region ensures the formation of the direct gaps of the prepared films. The following expression was used to find it [73-77]:

$$\alpha h\nu = A(h\nu - Eg)^{1/2} \quad (4)$$

hν: photon energy α: Absorption coefficient, and A: constant. To find the energy gap Eg accurately, a straight line of the $(\alpha h\nu)^2$ versus hν plot with the photon's energy [78, 79].

Figure 4 illustrates the absorption peak location at 320 nm in the 300 nm to 1100 nm absorption spectrum; the shift in the absorption peak towered the blue region indicates the GaN particles' Nano size (Figure 4). Lower broadening is observed in the spectrum absorption experimental data, and higher absorption implies a more significant concentration of GaN NPs.

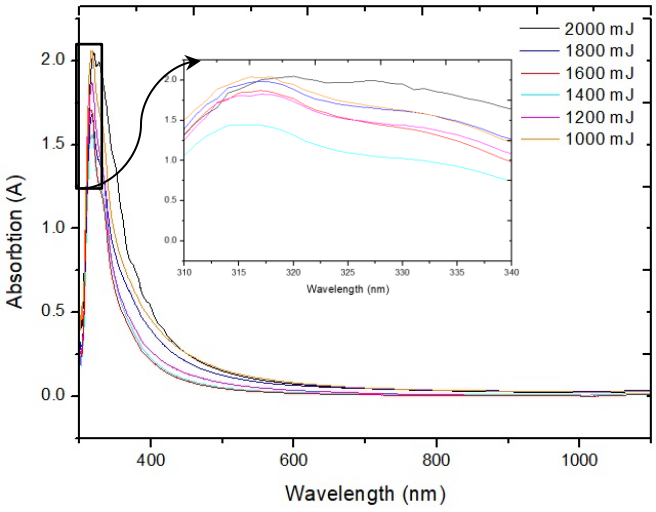

FIGURE 4. Absorption properties of GaN

The transmission curve of GaN at various deposition energies, ranging from maximum to minimum, is shown in Figure 5. The transmission value ranges from 86 to 93 percent in the visible spectrum. The granular size of the Nano colloidal, which was generated with varying laser

Note: Accepted manuscripts are articles that have been peer-reviewed and accepted for publication by the Editorial Board. These articles have not yet been copyedited and/or formatted in the journal house style.

intensity, caused the disparity in proportions. Transmission values were poor when using high power ablation such as 2000 mJ and 1800 mJ because of the large particle size and random and uneven distribution of the removed granules inside the liquid. Because of the tiny particle size and homogeneous distribution of the Nano colloidal particles, the rise in transmission values was visible when the laser ablation energy was lowered to 1400 mJ, where the greatest value of transmission emerged. The transmitter values begin to slowly fall again due to the weak laser energy's effect on the randomly damaged crystals and the poor dispersion within the liquid.

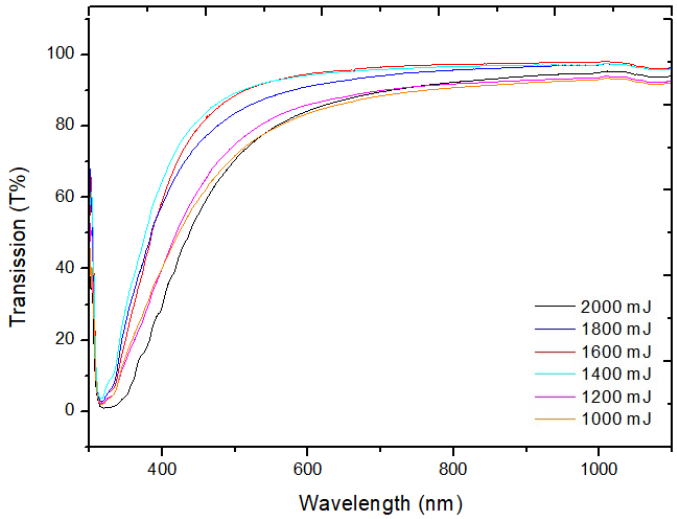

FIGURE 4. transmission curve of GaN at different laser deposition energy

As demonstrated in Figure 6, increasing the ablation energy will eliminate the larger partial size. As a result, the energy gap narrows, and the wavelength redshifts; lowering the ablation energy decreases particle size while increasing the energy gap. The wavelength will blue-shift until 1400mJ, when the maximum energy gap (3.62ev) is reached, after which the energy gap will decrease between 1200 and 1000 mJ, causing the wavelength to redshift owing to the core-shell phenomenon, increasing particle size. The best transmission values were at energies 1400 and 1600 mJ due to the best removal rate and an orderly distribution inside the colloidal liquid as the most petite sizes of nanoparticles.

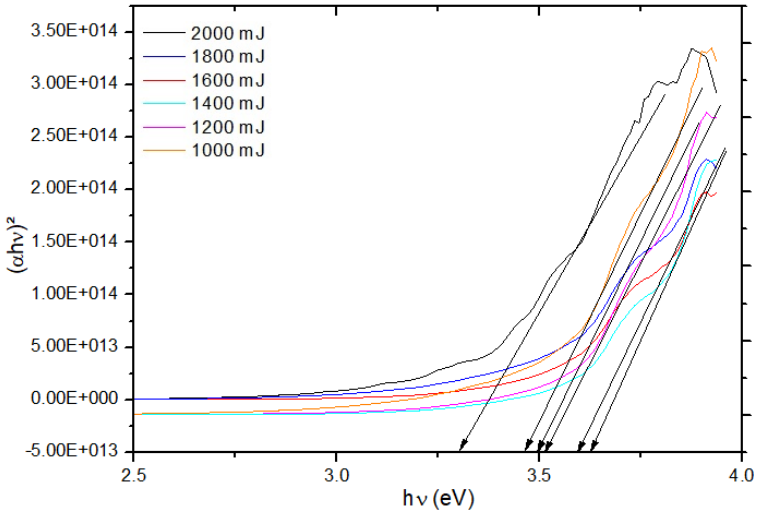

FIGURE 6. Energy gap of GaN at different laser deposition energy

4- CONCLUSIONS

Note: Accepted manuscripts are articles that have been peer-reviewed and accepted for publication by the Editorial Board. These articles have not yet been copyedited and/or formatted in the journal house style.

Pulsed laser ablation was used to grow high-quality thin-film GaN nanoparticles. The optical characteristics of GaN placed on a quartz substrate are examined using XRD, TEM, and UV-Vis absorption experiments in this work. First, the XRD test reveals that all presented diffraction peaks have a narrow FWHM magnitude of 0.12. The high-order GaN diffraction peak demonstrates excellent GaN thin film characteristics grown on the quartz substrate. Second, the TEM test revealed nanoparticles dispersed at the matrix, with the image representing all recognized peaks (reflection peaks) possibly indexed to hexagonal GaN structure. Finally, the UV-Vis absorption test reveals an absorption peak at 320 nm. A lesser broadening in the absorption spectrum experimental data and greater absorption implies a larger concentration of GaN NPs. The sharp point on the absorption coefficient curve indicates that there is insufficient energy in the material to excite an electron from one level to another. Also, the transmission value ranged from 86 to 93 percent, which also showed that the best transmission values were at energies 1400 and 1600 mJ. The bandgap value of the deposited Nano GaN films grows as the laser ablation energy decreases access to 1400 mj; the results of the optical bandgap ranged between 3.3 ev and 3.62 ev, where the best result was when using 1400 mJ ablation energy. A shift towered over the blue area in GaN nano-films created at a low laser wavelength. The possibilities of employing the generated thin Nano-films in optoelectronics applications such as optical detectors, solar cells, and optical sensors were evident from the findings obtained.

REFERENCES

[1] Ya-Qing, B., Zhi-Min, L., Hong-Zhou, Z., Guang-Ru, L., Yu, Y., Yang-Bo, Z., Jun, X., Zhi-Xin, Q., Lun, D., Da-Peng, Y., Adv. Mater. **23(5)** (2011) 649–653.

[2] Kris, A. B.,Aric, W. S., Devin, M. R., Todd, E. H., Alexana, R., John B. S., Norman, A. S., Adv. Funct. Mater. **20(17)** (2010) 2911–2915.

[3] Faisal, A. D., Ismail, R, A., Khalef, W, K., Salim, E. T., Optical and Quantum Electronics, **52** (2020) 1-12.

[4] Devan, R. S., Patil, R. A., Lin, J., and Ma, Y., Adv. Funct. Mater. **22(16)** (2012) 3326–3370.

[5] Kim, H. W., Kebede, M. A., and Kim, H. S., Vacuum **84(1)** (2009) 254–257.

[6] Salim, E.T., Saimon, J.A., Abood, M.K., Fakhri, M.A, Optical and Quantum Electronics, **52(10)** (2020) 463.

[7] Hassan, N. K., and Hashim, M. R., J. Alloys Compd. **577** (2013) 491–497.

[8] Wu, Q., Hu, Z., Wang, X., Hu, Y., Tian, Y., and Chen, Y., Diam. Relat. Mater., **13(1)** (2004) 38–41.

[9] Asady, H., Salim, E. T., Ismail, R. A., AIP Conference Proceedings, **2213(1)** (2020) 020183.

[10] Pan, X., Wei, M., Yang, C., Xiao, H., Wang, C., and Wang, X., J. Cryst. Growth **318(1)** (2011) 464–467.

[11] Feng, Z. C., Yang, T.-R., and Hou, Y. T., Mater. Sci. Semicond. Process. **4(6)** (2001) 571–576.

[12] Salim, E. T., Fakhri, M. A., Tareq, Z. T., Hashim, U., AIP Conference Proceedings, 2213(1) (2020) 020230.

[13] Saron, K. M. A., Hashim, M. R., Qaeed, M. A., Al-heuseen, K., and Elfadill, N. G., Mater. Sci. Semicond. Process. **29** (2015) 106–111.

[14] Pang, L., and Kim, K. K., Mater. Sci. Semicond. Process. **29** (2015) 90–94.

[15] Awayiz, M. T., Salim, E. T., AIP Conference Proceedings, **2213(1)** (2020) 020247.

[16] Yusoff, M. Z. M., Hassan, Z., Ahmed, N. M., Hassan, H. A., Abdullah, M. J., and Rashid, M., Mater. Sci. Semicond. Process., **16(6)** (2013) 1859–1864.

Note: Accepted manuscripts are articles that have been peer-reviewed and accepted for publication by the Editorial Board. These articles have not yet been copyedited and/or formatted in the journal house style.

[17] Pérez-Tomás, A., Fontserè, A., Jennings, M. R. and Gammon, P. M., Mater. Sci. Semicond. Process., **16(5)** (2013) 1336–1345.
[18] Fakhri, M. A., Salim, E. T., Abdulwahhab, A. W., Hashim, U., Minshid, M. A., Salim, Z. T., Surface Review and Letters, **26(10)** (2019) 1950068.
[19] Qiang, H.,Tongbo, W., Ruifei, D., Jiankun, Y., Ziqiang, Huo., Yiping, Z., Shu, X., Mater. Sci. Semicond. Process., **15(1)** (2012) 15–19.
[20] Joshi, B. C., Mathew, M., Joshi, B. C., Kumar, D., and Dhanavantri, C. Pramana, **74(1)** (2010) 135–141.
[21] Salim, E. T., Ismail, R. A., Halbos, H. T., Materials Research Express, **6(11)** 116429 (2019).
[22] Mantarc, A., Kundakç, M., AIP Conf. Proc., **1833(1)** (2017) 020119.
[23] Fong, C.Y., Ng, S.S., Yam, F.K., Abu Hassan, H., Hassan, Z., Vacuumm, **119** (2015) 119–122.
[24] Kawwam, M., Lebbou, K., Appl. Surf. Sci., **292** (2014) 906–914.
[25] Braniste, T., Ciers, J., Monaico, E., Martin, D., Carlin, J.F., Ursaki, V.V., Sergentu, V.V., Tiginyanu, I.M., Grandjean, N., Superlattice and Microst., **102** (2017) 221–234.
[26] Gu, S., Chagarov, E.A., Min, J., Madisetti, S., Novak, S., Oktyabrsky, S., Kerr, A.J., Kaufman-Osborn, T., Kummel, A.C., Asbeck, P.M., Appl. Surf. Sci., **317** (2014) 1022–1027.
[27] Wang, M., Bian, J., Sun, H., Liu,W., Zhang, Y., Luo, Y., Appl. Surf. Sci., **389** (2016) 199–204.
[28] Erdoğan, E., Kundakçı, M., Mantarcı, A., Journal of Physics Conference Series, **707(1)** (2016) 012019
[29] Kundakçı, M., Mantarcı, A., Erdoğan, E., Mater. Res. Exp., **4(1)** (2017) 016410
[30] M.-W. Ha, S.-C. Lee, S.-S. Kim, C.-M. Yun, and M.-K. Han, Superlattices Microstruct., **4(4–6)** (2006) 562–566.
[31] Qaeed, M. A., Ibrahim, K., Saron, K. M. A.. and Salhin, A. Superlattices Microstruct., **64** (2013) 70–77.
[32] Chen, Q., Yang, J.W., Gaska, R., Khan, M.S, Sullivan, G.J., Sailor, A.L., Higgings, J.A., Ping, A.T., Adesida, I. IEEE Electron Device Lett., **19(2)** (1998) 44–46.
[33] Pengelly, R. S., Wood, S. M., Milligan, J. W., Sheppard, S. T., and Pribble, W. L., IEEE Trans. Microw. Theory Tech., **60(6)** (2012) 1764–1783.
[34] Asgari, A., Karamad, M., and Kalafi, M., Superlattices Microstruct., **40(4–6)** (2006) 603–606.
[35] Shin, M. J., Kim, M., Lee, G. S., Ahn, H. S., Yi, S. N., and Ha, D. H., Mater. Lett., **91** (2013) 191–194.
[36] Kobayashi, N. and Kobayashi, Y., Appl. Surf. Sci., **159** (2000) 398–404.
[37] Grahn, H. T., Phys. status solidi, **241(12)** (2004) 2795–2801.
[38] Li, L.,Liu, L.,Wang, L.,Li, D.,Song, J.,Liu, N.,Chen, W.,Wang, Y.,Yang, Z.,Hu, X., Appl. Phys. A, **108(4)** (2012) 857–862.
[39] Yamada, A., Ho, K. P., Maruyama, T., and Akimoto, K., Appl. Phys. A, **69(1)** (1999) 89–92.
[40] Wang, J. C., Feng, S. Q., and Yu, D. P., Appl. Phys. A, **75(6)** (2002) 691–693.
[41] Cai, X.M. Wang, Y. Li, Z.D., Lv, X.Q., Zhang, J.Y., Ying. L.Y., Zhang, B.P., Appl. Phys. A, **111(2)** (2013) 483–486.
[42] Jiang, L. J., Wang, X. L., Xiao, H. L., Wang, Z. G., Yang, C. B., and Zhang, M. L. Appl. Phys. A, **104(1)** (2011) 429–432.
[43] Park, J. B., Kim, N.-J., Kim, Y.-J., Lee, S.-H., and Yi, G.-C., Curr. Appl. Phys., **14(11)** (2014) 1437–1442.
[44] Sharma, S. K., Heo, S., Lee, B., Lee, H., Kim, C., and Kim, D. Y. Curr. Appl. Phys., **14(12)** (2014) 1696–1702.

Note: Accepted manuscripts are articles that have been peer-reviewed and accepted for publication by the Editorial Board. These articles have not yet been copyedited and/or formatted in the journal house style.

[45] Bak, S. J., Mun, D. -H., Jung, K. C., Park, J. H., Bae, H. J., Lee, I. W., Ha, J. -S., Jeong, T., Oh, T. S., Electron. Mater. Lett., **9(3)** (2013) 367–370.
[46] Lee, Y. S., Seo, T. H., Park, A. H., Lee, K. J., Chung, S. J., and Suh, E.-K., Electron. Mater. Lett., **8(3)** (2012) 335–339.
[47] Vinegoni, C., Cazzanelli, M., Trivelli, A., Mariotto, G., Castro, J., Lunney, J.G., Levy, J., Surf. Coatings Technol., **124(2–3)** (2000) 272–277.
[48] Vispute, R. D.,Talyansky, V., Sharma, R. P., Choopun, S., Downes, M., and Venkatesan, T., Appl. Phys. Lett., **71(1)** (1997) 102–104.
[49] Goswami, L., Pandey, R., and Gupta, G., Appl. Surf. Sci., **449** (2018) 186–192.
[50] Pal, Y., Raja, M. A., Madhumitha, M., Nikita, A., and Neethu, A., Optik, **226** (2021) 165410.
[51] Choi, J.-H., Jang, S.-H., and Jang, J.-S., Electron. Mater. Lett., **9(4)** (2013) 425–428.
[52] Lin, Y. C., Liu, Y. S., Chang, C. L., and Liu, C. Y., Electron. Mater. Lett., **9(4)** (2013) 441–444.
[53] Glukhanyuk, V., Przybylińska, H., Kozanecki, A., and Jantsch, W., Opt. Mater. (Amst)., **28(6–7)** (2006) 746–749.
[54] Guillermo, S., Osvaldo, D. M., Jorge, A. g., Rogelio, M., Marel, M. B., Adolfo, E., Máximo, López-López., Francisco, D. M.,Luis, A. H., and Gerardo, C., Materials (Basel)., **6(3)** (2013) 1050–1060.
[55] Contreras-Puente, G., Cantarero, A., Recio, J. M., Melo, O., Hernández-Cruz, E., Flores, F. d. M., Mendoza-Pérez, R., in **2012** 38th IEEE Photovoltaic Specialists Conference, (2012) 36–38.
[56] Husam, A. A. A, Fakhri, M.A. Alwahib, A A., Materials Today: Proceedings, **42** (2021) 2815-2821.
[57] Fakhri, M. A., Salim, E. T., Wahid, M. H. A., Salim, Z. T., Hashim, U., AIP Conference Proceedings, **2213(1)** (2020) 020242.
[58] Mahdi, R. O., Fakhri, M. A., Salim, E. T., Materials Science Forum **1002** (2020) 211-220.
[59] Jabbar, H.D., Fakhri, M.A., Abdulrazzaq, M. J., Materials Today: Proceedings, **42(5)** (2021) 2829-2834.
[60] Awayiz, M. T., Salim, E. T., Materials Science Forum, **1002** (2020) 200-210.
[61] Claudio, V., Massimo, C., Trivelli, A., Gino, M., Juan, F. C., Lunney, J.G., Jeremy, L. Surf. Coatings Technol., **124(2–3)** (2000) 272–277.
[62] Vispute, R. D., Talyansky, V., Sharma, R. P.,Choopun, S., Downes, M., and Venkatesan, T., Appl. Phys. Lett., **71(1)** (1997) 102–104.
[63] Schulz, H., Thiemann, K.H., Solid State Commun. **23(11)** (1977) 815–819.
[64] Yeh, C., Lu, Z.W., Froyen, S., Zunger, A., Phys. Rev. B. **46(16)** (1992) 10086–10097.
[65] Abood, M., Salim, E. T., Saimon, J, A., Journal of Ovonic Research, **15(2)** (2019) 109 – 115.
[66] Fakhri, M. A., Salim, E. T., Wahid, M. H. A., Abdulwahhab, A. W., Salim, Z. T., Hashim, U., Journal of Physics and Chemistry of Solids, **131** (2019) 180-188.
[67] Alwahib, A. A., Al-Rekabi, S. H., and Muttlak, W. H., AIP Conf. Proc., **2213** (2020) 020143, (2020).
[68] Orak, I., Kocyigit, A., Turut, A., J. Alloys Compd. **691** (2017) 873–879.
[69] Gao, X. Y., Wang, S., Li, J., YX Zheng, R. J. Zhang, Zhou, P., Yang, Y. M., Chen, L. Y., J. Korean Phys. Soc., **44(3 II)** (2004) 765–768.
[70] Yoshida, T., Kakumoto, S., Sugimura, A., and Umezu, I., Appl. Phys. A, **104(3)** (2011) 907–911.

Note: Accepted manuscripts are articles that have been peer-reviewed and accepted for publication by the Editorial Board. These articles have not yet been copyedited and/or formatted in the journal house style.

[71] Bragg, W. H., and Bragg, W. L., Proceedings of the Royal Society of London. Series A, **88(605)** (1913) 428-438.
[72] Mantarc, A. & Kundakçi, M., Journal of the Australian Ceramic Society, **56** (2020) 905–914.
[73] Velazquez, R., Aldalbahi, A., Rivera, M., and Feng, P., AIP Advances, **6** (2016) 085117.
[74] Nasr, F. B., Guermazi, H., and Guermazi, S., Eur. Phys. J. Plus, **131** (2016) 195.
[75] Alwahib, A. A., Alhasan, S. F., Yaacob, M. H., Lim, H. N., and Mahdi, M. A., Optik (Stuttg)., **202** (2020) 163724.
[76] Salim, E. T., Hassan, A. I., Naaes, S. A., Materials Research Express, **6(8)** (2019) 086416.
[77] Alwahib, A. A., Muttlak, W. H., and Abdulhadi, A. H., Int. J. Nanoelectron. Mater., **12(2)** (2019) 145–156.
[78] Fakhri, M. A., AbdulRazzaq, M. J., Alwahib, A. A., Muttlak, W. H., Optical Materials **109** (2020) 110363.
[79] Abed, A. L., Khalef, W.K., Salim, E.T., Journal of Physics: Conference Series, **1795(1)** (2021) 012031

Note: Accepted manuscripts are articles that have been peer-reviewed and accepted for publication by the Editorial Board. These articles have not yet been copyedited and/or formatted in the journal house style.